Block Copolymer Solutions under External Electric Field: Dynamic Behavior Monitored by Light Scattering

Fernando C. Giacomelli, Izabel C. Riegel,† Cesar L. Petzhold, and Nádya P. da Silveira*

Instituto de Química, Universidade Federal do Rio Grande do Sul, Av. Bento Gonçalves 9500, 91501-970 Porto Alegre, Brazil

Received October 26, 2007; Revised Manuscript Received January 16, 2008

ABSTRACT: A home-built capacitor was constructed in order to study the influence of an external electric field in polymer solutions by means of light scattering measurements. Herein, solutions of a triblock copolymer made of styrene and 5-*N,N*-(diethylamino)isoprene (PAI_{11}-*b*-PS_{228}-*b*-PAI_{11}) in pure THF, DMF, or cyclohexane were studied. In THF, only random coil structures ($R_h \sim 3.6$ nm) were identified, which were not affected by the applied electric field in the range studied (up to 225 kV m^{-1}). In DMF, micelles having R_h around 25 nm have self-formed, and their diffusion constant has increased linearly with the square of the applied electric field. The observed effect was attributed to the generation of a dipole moment on the micelles. In cyclohexane, huge aggregates R_h around 100 nm and free chains were detected. In this case, the induced dipole moment has the same direction of the electric field, favoring electrostatic interactions between the structures, since it was observed that the clusters dimensions have increased as a function of applied electric field time. As a consequence of the attractive forces, clusters amount in solution has decreased, which is supposed to be related to a precipitation process.

Introduction

One of the most attractive properties of amphiphilic block copolymers is their ability to form organized structures in solution. When these materials are dissolved in a thermodynamically good solvent for only one block, self-aggregates may be expected,[1,2] and a wide range of morphologies in solution can be achieved altering the molecular weight, block length, and nature as well as the method of dissolution. Vesicles,[3–5] micelles,[6] and hollow spheres[7] are some of the most reported cases. These self-formed objects are of great importance in the transport of small molecules, especially in the drug delivery field.

Because of their very interesting properties and the growing interest in potential applications, the study of the dynamic behavior of self-formed block copolymer nanostructures, in liquid media, is of noteworthy importance. Furthermore, employment of external forces can be used to manipulate the diffusion constants of the formed polymeric structures throughout different fluids, accelerating or delaying some processes, as well as can interfere in their structural reorganization in solution.

A large number of contributions can be found focusing on the application of external electric fields in bulk and thin films block copolymers. Most of them aim at order–disorder and order−order phase transitions investigations[8–13] as well as phase separation processes.[14,15] Electric fields have also been applied in block copolymer solutions intending structure alignment. Krausch et al. demonstrated the alignment, by electric field, of large-scale domains of highly concentrated block copolymers solutions,[16–18] employing small-angle X-ray measurements. Putaux et al., using light microscopy, have studied the alignment of cellulose fibers suspended in toluene when an external electric field was applied through the system.[19] Moreover, Li et al. verified, using transmission and scanning electron microscopies, that by applying an alternating electric field, highly long-range ordered aggregates are generated from PS−PAA micelles in aqueous solution.[20]

On the other hand, the behavior of polymer solutions under external electric fields has rarely been studied by light scattering (LS) measurements. In the literature, just a few experimental works dealing with polystyrene were found.[21–23] The reasons are essentially related to the difficulties to prepare a reliable experimental setup to hinder light reflections and the need to avoid electrophoretic effects, which is possible only when the studied systems have some special characteristics.[24] Nevertheless, LS is one of the best techniques to study dynamic processes in solution since a large number of particles can scatter independently regarding the scattering volume is sufficiently large.

The motivation of the present contribution was to study the changes provoked by an external electric field in the dynamic behavior of a block copolymer in solution using static (SLS) and dynamic light scattering (DLS). The application of external electric fields across the organic polymer solutions was achieved through a home-built capacitor, made of inert materials. A coherent geometry was used to build up the capacitor in order to avoid unexpected light reflections. Solutions of a triblock copolymer of styrene (PS) and 5-*N,N*-(diethylamino)isoprene (PAI) were prepared by simply dissolving the material in selective (good solvent for one block and poor for the other) and nonselecting (good for both blocks) solvents, in order to induce self-aggregates with different sizes and morphologies. Dimethylformamide (DMF), a selective solvent for PS, cyclohexane (CH), a selective solvent for PAI, and tetrahydrofuran (THF), which is considered a good solvent for both blocks, were used. Self-formed aggregates were studied under a direct current (dc) external electric field applying varied intensities.

Experimental Section

Chemicals. The highly asymmetric triblock copolymer sample PAI_{11}-*b*-PS_{228}-*b*-PAI_{11} ($M_n = 26\,800$ g mol^{-1} and $M_w/M_n = 1.20$) was synthesized via sequential anionic polymerization. Its molecular structure is depicted in Figure 1. The detailed synthesis procedure as well as preliminary characterization can be found elsewhere.[25]

Polymer solutions were prepared using solvents of analytical grade (THF, DMF, CH) purchased from Aldrich and used without further purification.

* Corresponding author: e-mail nadya@iq.ufrgs.br; Tel +55 51 33087321; fax +55 51 33087304.

† Current address: RS 239, 2755 Centro Universitário Feevale, Novo Hamburgo, RS, Brazil.

10.1021/ma7023792 CCC: $40.75
Published on Web 03/07/2008

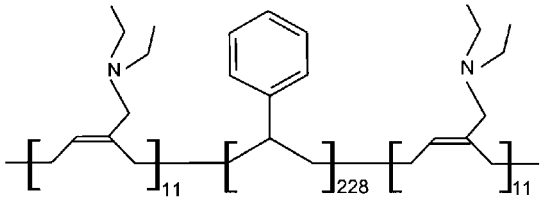

Figure 1. Molecular structure of PAI_{11}-*b*-PS_{228}-*b*-PAI_{11}.

Table 1. Physical Parameters of the Organic Solvents at 20 °C[26] [a]

solvent	viscosity (mPa·s)	RI	δ (MPa)$^{1/2}$	ϵ
DMF	0.55	1.407	18.6	36.70
THF	0.92	1.431	24.8	7.52
CH	0.98	1.426	16.8	2.02

[a] RI = refractive index; δ = solubility parameter; ϵ = dielectric constant; THF = tetrahydrofuran; DMF = dimethylformamide; CH = cyclohexane.

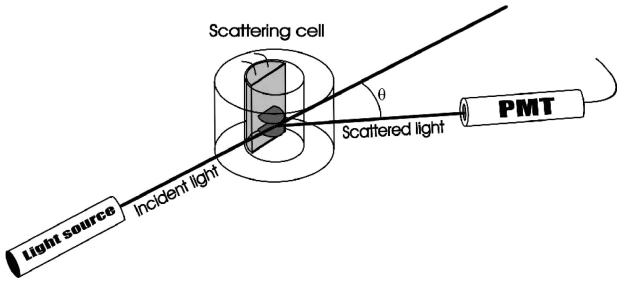

Figure 2. View of the scattering cell configuration; PMT is a photomultiplier tube.

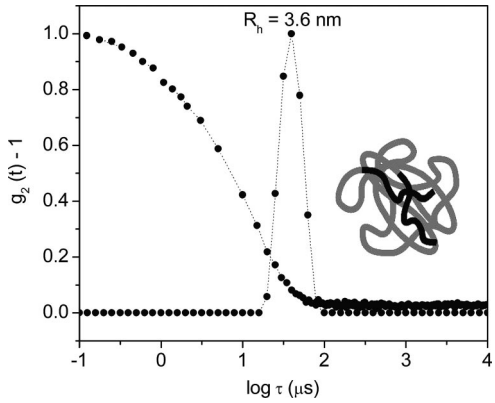

Figure 3. Autocorrelation function measured at scattering angle of 90° and distribution of the relaxation times revealed by REPES analysis for a 0.5 wt % solution of PAI_{11}-*b*-PS_{228}-*b*-PAI_{11} in THF, when the electric field was switched off. The inset represents the triblock copolymer as a random coil.

Samples Preparation. The samples were obtained by using the single-solvent dissolving method, wherever a certain amount of the polymer (0.5 wt %) was dissolved in the organic solvents and the resulting solutions were kept under gently stirring overnight, at room temperature. After the dissolution step, samples were filtered through suitable Millipore filters with pore sizes of 0.45 μm and transferred to the couvette containing the capacitor. Besides their distinct solubility parameters, these solvents were also selected due to their distinct dielectric constants (given in Table 1).

Electric Field Application. A dc external electric field was applied to the solutions using a home-built capacitor schematically represented in Figure 2.

As shown, the electric field is perpendicular to the beam light, allowing the scattered light detection in a large angle range. The capacitor was constructed using a polyacetal remnant as support for two parallel circular copper plates (electrodes) with a black finish to avoid undesirable light reflections. The electrodes separation was chosen as 4 mm. External dc electric fields, up to 225 kV m^{-1}, were applied using a high-power voltage supply (Ortec, model 456). During the experiments the temperature, the applied voltage, and the current density were carefully monitored.

Light Scattering Measurements. The measurements were performed at room temperature (20 ± 1 °C) using a Brookhaven Instruments standard setup (BI200 M goniometer, BI9000AT digital correlator) with a vertically polarized Coherent He−Ne Laser (λ = 632.8 nm) as light source. The scattering volume was minimized using a 0.4 mm aperture and an interference filter before the entrance of the photomultiplier. Polarized homodyne intensity autocorrelation functions $g_2(t)$ were obtained using a multi-τ mode correlator with 224 channels. The scattered light was analyzed after placing the sample cell containing the apparatus in decahydronaphthalene (Aldrich), which is an index-matching liquid.

Data Analysis. Normalized electric field correlation functions $g_1(t)$, calculated from the intensity autocorrelation functions $g_2(t)$, were analyzed by using the regularized positive exponential sum (REPES), which employs the Laplace inversion. The resulting $A(\tau)$ is a distribution of relaxation times:

$$g_2(t) - 1 = \beta\left[\int A(\tau)\exp(-t/\tau)\int d\tau\right]^2 \quad (1)$$

In eq 1, t is the delay time of the correlation function and β is a coefficient accounting from ideal correlation. The relaxation time τ or the relaxation frequency $\Gamma(\tau^{-1})$ is associated with a diffusion coefficient D through the relation

$$D = \frac{\Gamma}{q^2} \quad (2)$$

The scattering vector q takes into account the refractive index of the solvent (n) and the scattering angle (θ) as given in eq 3.

$$q = \frac{4\pi n}{\lambda}\sin\left(\frac{\theta}{2}\right) \quad (3)$$

The hydrodynamic radii (R_h) were then calculated from the diffusion coefficient using the well-known Stokes–Einstein equation:

$$R_h = \frac{k_B T}{6\pi\eta D} \quad (4)$$

wherein k_B is the Boltzmann constant, T is the absolute temperature, and η is the viscosity of the solvent.

The value of the radius of gyration (R_g) for micelles formed in DMF was determined using angular dissymmetry measurements. The intensity of light scattered becomes greater in the forward direction, relative to the backward one, when R_g of the scattering objects exceeds ~1/20 the wavelength of the incident beam. In these cases, the ratio between the intensity of scattered light in supplementary angles is related to R_g in the following way.[27]

$$\frac{I(\theta)}{I(180-\theta)} = 1 + \left(\frac{4\pi n}{2\lambda}\right)^2\left(\frac{R_g^2}{3}\right)\cos\theta \quad (5)$$

This is valid for $qR_g < 1$, and the linear slope of the curve gives the value of R_g.

Results and Discussion

Behavior in Polar Solvents (THF and DMF). Figure 3 shows a typical autocorrelation function, measured at scattering angle of 90°, and the distribution of relaxation times, revealed by REPES analysis, for a solution of 0.5 wt % PAI_{11}-*b*-PS_{228}-*b*-PAI_{11} in THF when the electric field was switched off.

Only a single narrow distribution was observed comprising a roughly 3.6 nm mean hydrodynamic radius (R_h). Keeping in mind that the average unperturbed end-to-end distance of a C−C polymer chain is equal to the length of one repeat unit multiplied

by the square root of the number of repeating units[28] as demonstrated by the equation

$$\langle r \rangle = l\sqrt{N} \tag{6}$$

where $l \sim 2.5$ Å and $N \sim 250$, the theoretical value of the end-to-end distance for PAI_{11}-*b*-PS_{228}-*b*-PAI_{11} was calculated to be ~4.0 nm. This value is very close to the experimental value of R_h determined, enlightening that, in THF and in this regime of concentration, PAI_{11}-*b*-PS_{228}-*b*-PAI_{11} exists as free chains in solution. When this solution was submitted to an external electric field, the values of the relaxation frequency, related to the free chains motion, did not change significantly. Values in the range of 51–53 ms^{-1} were found when applying an external electric field from zero (switched off) up to 75 kV m^{-1}.

Figure 4 shows a typical autocorrelation function, measured at scattering angle of 90°, and the distribution of the relaxation times, revealed by REPES analysis, for a solution of 0.5 wt % PAI_{11}-*b*-PS_{228}-*b*-PAI_{11} in DMF, when the electric field was switched off.

A relatively narrow distribution was also found in DMF. However, the structures in solution have a mean hydrodynamic radius of 25 nm. Since DMF is considered a thermodynamically good solvent for PS and a precipitant for PAI, this highly asymmetric block copolymer should form micelles when dissolved in DMF due to a series of thermodynamic factors.[29,30] Thus, it is expected that PAI_{11}-*b*-PS_{228}-*b*-PAI_{11} self-assemblies in structures containing a rigid PAI core and a PS corona, as schematically represented in the inset of Figure 4. The calculated dimensionless ratio $\rho = R_g/R_h$, which has been applied as a sensitive index of conformation of scattering objects, supports the above considerations. The radius of gyration (R_g) was determined for the self-formed structures using the dissymmetry method, and a value of 21.5 nm was found. Therefore, a ρ value in the vicinity of 0.8 was obtained, suggesting the formation of spherical homogeneous aggregates (classical micelles) since the theoretical value of ρ for solid spheres is about 0.778.[31] The average aggregation number determined from static light scattering measurements is around 35–40 chains per micelle.

Electric fields up to 75 kV m^{-1} were then applied to the DMF solution. The determined relaxation frequency (at $\theta = 90°$) characteristic from micelles motion was equal to 1.42 ms^{-1}. This value shifted to 5.38 ms^{-1} when the highest electric field was applied. Likewise, Figure 5 shows how the profile of q^2 dependence of Γ is modified in this system when the electric field is switched on.

The applied electric field produces at least two different effects. First, although the typical linear q^2 dependence of Γ is preserved, a linear coefficient also comes out. The curves can

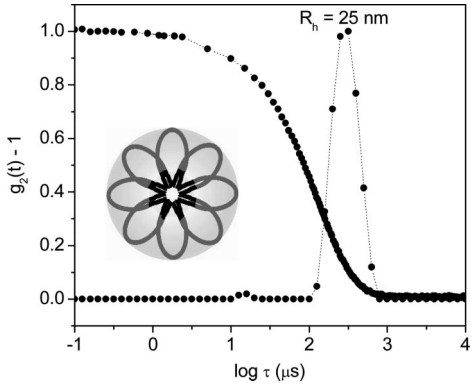

Figure 4. Autocorrelation function measured at scattering angle of 90° and distribution of the relaxation times revealed by REPES analysis for 0.5 wt % PAI_{11}-*b*-PS_{228}-*b*-PAI_{11} in DMF in the absence of an electric field. The inset depicts the triblock copolymer as an aggregate in DMF.

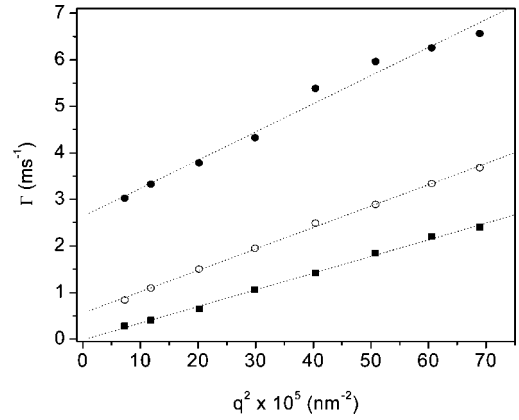

Figure 5. Relaxation frequencies (Γ) plotted against the square of the scattering vector (q^2) for a 0.5 wt % solution of PAI_{11}-*b*-PS_{228}-*b*-PAI_{11} in DMF, under electric fields of different intensities: switched off (■), 37.5 kV m^{-1} (○), and 75.0 kV m^{-1} (●).

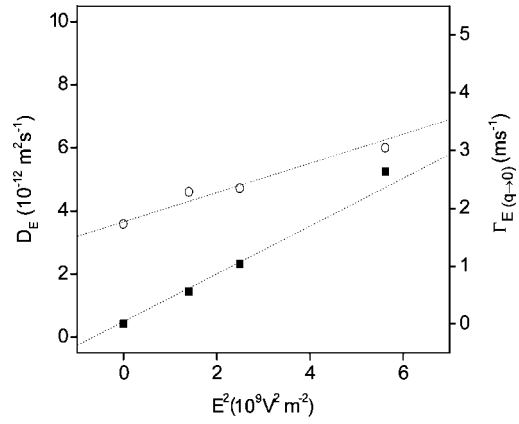

Figure 6. Dependence of D_E (○)and $\Gamma_{E(q\to0)}$ (■) on E^2 (electric field applied in a 0.5 wt % PAI_{11}-*b*-PS_{228}-*b*-PAI_{11} DMF solution).

be fitted by the relation $\Gamma_E = \Gamma_{E(q\to0)} + D_E q^2$ under this condition. Furthermore, the apparent diffusion coefficient of the micelles, given by the slope of the curves, and the value of the emerged pure frequency ($\Gamma_{E(q\to0)}$) increase following an E^2 dependence, as can be verified in Figure 6.

The distinct behaviors considering primarily the diffusional dynamics of the scattering objects immersed in THF and DMF can be understood taking into account the contributions of both energies: the thermal one, which is independent of the electric field, and the additional electric energy, which is promoted by the electric field. Classically, particles organized in a nanoscale domain move in a continuous media governed by Brownian motion. Their diffusion constant in absence of external fields is characterized by a relaxation frequency (Γ), which is determined in DLS measurements using the Stokes–Einstein relationship for diffusion of spherical particles in a viscous media ($\Gamma \propto D$, eq 2). Hence, the thermal energy of the system given by

$$E_{\text{Thermal}} = k_B T \tag{7}$$

is the responsible for the particles dynamics. Moreover, when submitted to an external electric field (E), an induced dipole moment (p) is generated in these particles of radius R, ascribed quantitatively as[32]

$$p = 4\pi\epsilon\epsilon_0\beta R^3 E \tag{8}$$

where ϵ_0 is the permittivity of the free space (8.854×10^{-12} F m^{-1}) and β is a dielectric mismatch parameter that involves the dielectric constant of the particles. Considering the dielectric

constant of micelles equals the dielectric constant of PS as an approximation in our case (ϵ_{PS}), and the dielectric constant of the solvent (ϵ_S), β can be described through the relation

$$\beta = \frac{\epsilon_{PS} - \epsilon_S}{\epsilon_{PS} + 2\epsilon_S} \tag{9}$$

Thus, the dipole moment produces an electric energy ($E_{electric} = pE$) acting in the free chains and in the micelles, which can be described as

$$E_{electric} = 4\pi\epsilon\epsilon_0\beta R^3E^2 \tag{10}$$

Hence, the increase in the diffusion rate of the micelles might be related to the electric energy imposed to the system. A pronounceable and clear effect of the external electric field in DMF solution was possible to be monitored mainly due to the high dielectric constant of the solvent as well as to the relative huge size of the aggregates ($R_h = 25$ nm), since $E_{electric} \propto \epsilon R^3$. In THF, because of the small radius of the random coils ($R_h = 3.6$ nm) and relatively low dielectric constant of THF, when compared to DMF, the magnitude of the dipole moment induced in the free chains is insignificant with regard to the thermal energy already present. In THF, the electric energy acting in a random coil represents $\sim 1.5 \times 10^{-3}$% of the thermal one at 20 °C when $E = 75$ kV m^{-1}. In the same conditions, the energy produced by the dipole moment induced in the micelles from the DMF solution is nearly 4% of the thermal energy characteristic of this system.

Since $\beta < 0$ ($\epsilon_{DMF} > \epsilon_{PS}$) in the DMF solution, the dipole moment acquired by the micelles has an opposite direction related to the direction of the applied electric field, which is promoted by the solvent moieties surrounding them. Thus, micelles should experience a torque to overcome the unstable situation created as well as to align their dipole moment with the electric field.[32] However, as a consequence of this motion, the dipole moment and the electric field became normal to each other, causing a repulsion between micelles, as demonstrated in Figure 7.

This qualitative discussion can explain the absence of aggregation in the sample, since chains, such as should be found in an electrorheological fluid, could not be formed in the outlined setup. The interface polarization and therefore the repulsion between particles might have a noteworthy contribution on the rate of diffusion determined through the relaxation rates, resulting in the increase of the determined values of D_E. It is worth mentioning that the absolute scattering intensity coming from the solution remained constant during the whole period of experiments, independently of the electric field intensity, guiding as conclusion that the electric field is not high enough to change the random distribution of the particles and strongly suggesting the absence of a driving electrophoretic force leading to anisotropy. Actually, the behavior observed was expected having in mind the small size of the formed micelles which approaches nanoscale. Thus, the electric field influences the movement of these objects promoting interactions of generated dipoles; however, the Brownian motion is still predominant.

Conversely, the origin of the E^2 dependence in $\Gamma_{E(q\to 0)}$ values seems not to be linked to the particles diffusion, but instead, it should be related to the quality of the solvent (that is, to its dielectric constant). As far as we can tell, it may come from a spatially nonuniform electric field present in the "solution background", experienced by the solvent. Indeed, when the same range of electric fields has been applied to PMMA−PHSA hard spheres suspended in DMF as well as in other solutions of polymer liquid crystals in DMF, we obtained results that matches very well with the ones depicted in Figure 6 (namely, the origin of a pure frequency parameter on $q \to 0$ intercept in Γ vs q^2 curves, linearly dependent on E^2 and located in the same range of frequencies, from 0 to roughly 4 ms^{-1}).

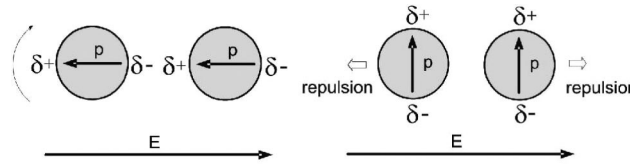

Figure 7. Cartoon illustrating the micelles behavior under an electric field for dielectric mismatch $\beta < 0$.

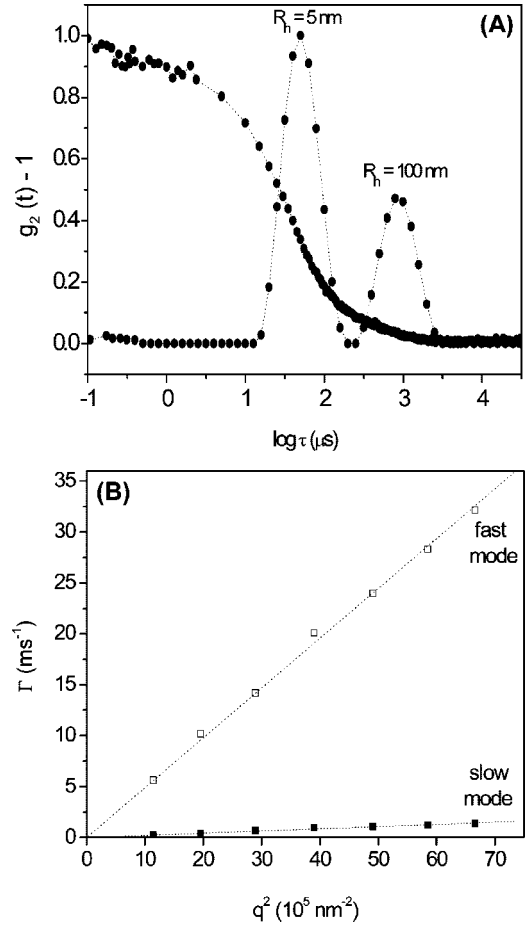

Figure 8. Autocorrelation function monitored at scattering angle of 90° and distribution of the relaxation times for 0.5 wt % PAI_{11}-*b*-PS_{228}-*b*-PAI_{11} cyclohexane solution (A) and Γ vs q^2 plots for the fast and slow modes found from data analysis (B).

Behavior in Apolar Solvent (Cyclohexane). The behavior of PAI_{11}-*b*-PS_{228}-*b*-PAI_{11} in cyclohexane was also studied under an external electric field.

Figure 8 shows the autocorrelation function and the distribution of the relaxation times for 0.5 wt % PAI_{11}-*b*-PS_{228}-*b*-PAI_{11} cyclohexane solution (A) and the Γ vs q^2 profiles of the two distributions observed (B). The heterogeneities were attributed to the formation of clusters as also reported in a previous paper,[33] knowing that cyclohexane is a relative poor solvent for PS. Even in low concentration (or diluted regime), the polymer chains tend to aggregate due to the weak polystyrene−solvent affinity.

Once an electric field is made to pass across the solution, only the larger structures are greatly affected by the electrostatic force in a manner completely different to that in DMF. Figure 9 shows the dependence of the relaxation rates against the square of electric field for the fast and slow modes in all range of applied electric field. Up to 100 kV m^{-1} ($E^2 = 10^{10}$ V^2 m^{-2}), the external force have not influenced the relaxation frequency values; i.e., the electric energy offered is insufficient to induce

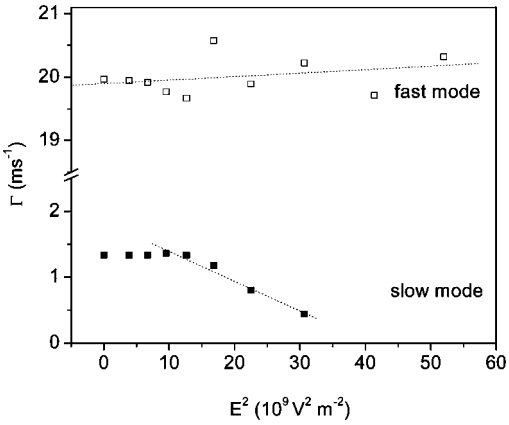

Figure 9. Γ vs E^2 plots for the fast and slow modes for 0.5 wt % PAI_{11}-*b*-PS_{228}-*b*-PAI_{11} cyclohexane solution. The autocorrelation functions were monitored at scattering angle of 90°.

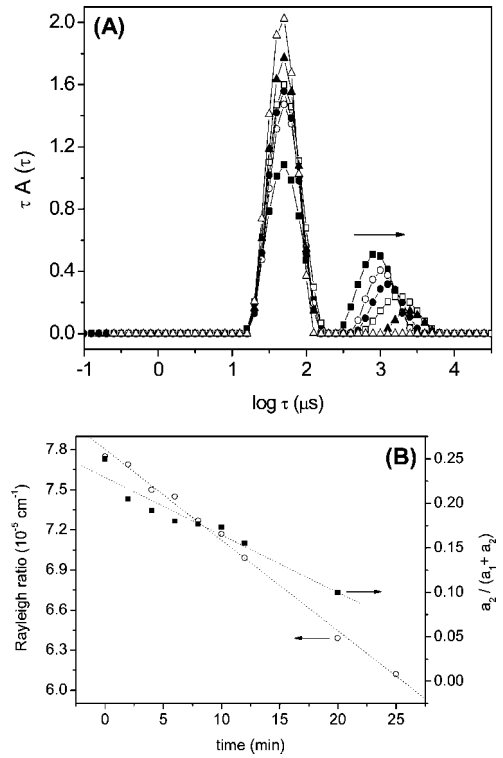

Figure 10. Distribution of the relaxation times as a function of time for a constant dc external electric field (225 kV m^{-1}) for 0.5 wt % PAI_{11}-*b*-PS_{228}-*b*-PAI_{11} cyclohexane solution: not applied (■), 2 min (○), 6 min (●), 12 min (□), 20 min (▲), and 25 min (△) in (A); Rayleigh ratio and amplitude of the cluster component (a_2) to the free chains polymer component (a_1), both as a function of time in (B).

changes. Nevertheless, higher intensities have a remarkable influence displacing Γ_{slow} to smaller values.

In order to better explain this event, autocorrelation functions were also monitored against time when a constant electric field (225 kV m^{-1}) was applied across the solution. They were recorded for 25 min at every few minutes. Distributions of the relaxation times obtained as a function of time are depicted in Figure 10A.

It was observed a displacement of the slow mode to higher times (smaller relaxation frequency values) with increasing time. Furthermore, the Rayleigh scattering of the solution and the relative amplitude of the cluster component decreased as a function of time (Figure 10B). According to these results, surely, the shift of the slow mode toward upper times can be attributed to an increase in the hydrodynamic mean radius of the clusters,

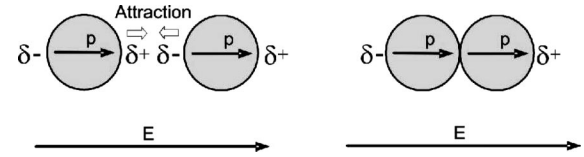

Figure 11. Cartoon illustrating the clusters behavior under an electric field for dielectric mismatch $\beta > 0$.

since changes in other physical parameters that could affect the dynamic behavior of the particles (namely temperature and mainly medium viscosity) would affect the relaxation rates of the fast mode as well. In this study, the relaxation rates of the fast mode did not change with time. The apparent R_h value of the large size clusters increases twice (from 100 to 200 nm) in 20 min, under a 225 kV m^{-1} applied electric field. Afterwards, REPES analysis was unable to resolve the slow mode due to the very low scattering intensity coming from the aggregates.

The increase in clusters dimension may came from their attraction. Cyclohexane has a dielectric constant equal to 2.02. The dielectric constant of the PS (main polymer component) is about 2.56. Unfortunately, this value is unknown for PAI, but certainly it is still higher than the PS value, according to the molecular structure of the PAI monomer. Thus, the β parameter has a positive value. Consequently, the dipole moment induced in the particles may have the direction of the electric field. Because of the small size of the free chains, the electric energy imposed does not affect their motion since the thermal energy is totally dominant (the ratio $E_{electric}/E_{thermal} = 2.87 \times 10^{-3}\%$ for an applied electric field of 225 kV m^{-1}). Conversely the dipole moment induced in the clusters engender a considerably electric energy ($E_{electric}/E_{thermal} \sim 2.3\%$), and this situation ($\beta > 0$) facilitates the attraction between neighbor clusters, leading to the formation of bigger aggregates, as shown in Figure 11.

This process of aggregation causes a reduction in the number of large particles diffusing in the scattering volume. Moreover, the reduction in their importance (a_2) in the distribution of relaxation times and also the reduction in the scattering intensity of the solution might be a consequence of their size increase. Probably, their density is also growing, leading at the same time to a process of precipitation which can explain the reduction in the scattering intensity, even with an enhancement in the size of the large particles, as a function of time.

Conclusions

Electric fields with varied intensities were applied across copolymer solutions, and the experimental results were understood considering the establishment of a dipole moment in the aggregates present in the liquid matrix. Electric field influence was detectable by means of dynamic light scattering measurements only when the electric energy imposed was sufficiently high (~3% of the thermal energy already present). Free chains dissolved in THF as well as in cyclohexane were not affected by the electric energy added due their small size ($E_{electric} \propto R^3$). An increment in the relaxation rates meaning a faster diffusion motion was observed in micelles formed in DMF emerging from repulsion forces between the aggregates. Additionally, a spatially nonuniform electric field is supposed to be taking place as a solution background, supported by the appearance of a linear coefficient in Γ vs q^2 curve profile.

A quite different behavior was observed in cyclohexane. The values of Γ for the slow mode (clusters motion) were displaced to smaller values when relative high electric fields were applied through the solution. However, in this case the effect was attributed to an increase in the cluster dimension due to mutual attraction. A precipitation process of the large particles following their size increase is supposed to be taking place due to the

observed reduction in the relative amplitude of the cluster component, revealed by REPES, and also in the average scattering intensity coming from the solution.

Acknowledgment. The authors thank CNPq for financial support and for the fellowship granted to F.C.G. The authors also thank Dr. Ricardo Rego Bordalo Correia and Ernesto Dornelles Pinto for helpful discussions.

References and Notes

(1) Hamley, I. W. *Block Copolymer in Solution: Fundamentals and Applications*; John Wiley: New York, 2006.
(2) Alexandridis, P.; Lindman, B. *Amphiphilic Block Copolymers: Self-assembly and Applications*; Elsevier: Amsterdam, 2000.
(3) Wittemann, A.; Azzami, T.; Eisenberg, A. *Langmuir* **2007**, *23*, 2224–2230.
(4) Opsteen, J. A.; Cornelissen, J. L. M.; van Hest, J. C. M. *Pure Appl. Chem.* **2007**, *76*, 1309–1319.
(5) Soo, P. L.; Eisenberg, A. *J. Polym. Sci., Part B: Polym. Phys.* **2004**, *42*, 923–938.
(6) Bhargava, P.; Zheng, J. X.; Li, P.; Quirk, R. P.; Harris, F. W.; Cheng, S. Z. D. *Macromolecules* **2007**, *39*, 4880–4888.
(7) Rahman, M. S.; Samal, S.; Lee, J. *Macromolecules* **2006**, *39*, 5009–5014.
(8) Amundson, K.; Helfand, E.; Quan, X.; Hudson, S. D. *Macromolecules* **1994**, *27*, 6559–6570.
(9) Ashok, B.; Muthukumar, M.; Russel, T. P. *J. Chem. Phys.* **2001**, *115*, 1559–1564.
(10) Matsen, M. W. *Macromolecules* **2006**, *39*, 5512–5520.
(11) Tsori, Y.; Andelman, D. *Macromolecules* **2002**, *35*, 5161–5170.
(12) Xu, T.; Zvelindovsky, A. V.; Sevink, G. J. A.; Gang, O.; Ocko, B.; Zhu, Y.; Gido, S. P.; Russel, T. P. *Macromolecules* **2004**, *37*, 6980–6984.
(13) Matsen, M. W. *J. Chem. Phys.* **2006**, *124*, 1–9.
(14) Hori, H.; Urakawa, O.; Yano, O.; Tran-Cong-Miyata, Q. *Macromolecules* **2007**, *40*, 389–394.
(15) Tsori, Y.; Tournilhac, F.; Leibler, L. *Nature (London)* **2004**, *430*, 544–547.
(16) Böker, A.; Schmidt, K.; Knoll, A.; Zettl, H.; Hansel, H.; Urban, V.; Abetz, V.; Krausch, G. *Polymer* **2006**, *47*, 849–857.
(17) Böker, A.; Knoll, A.; Elbs, H.; Abetz, V.; Muller, A. H. E.; Krausch, G. *Macromolecules* **2003**, *35*, 1319–1325.
(18) Böker, A.; Elbs, H.; Hansel, H.; Knoll, A.; Ludwigs, S.; Zettl, H.; Urban, V.; Abetz, V.; Muller, A. H. E.; Krausch, G. *Phys. Rev. Lett.* **2002**, *89*, 1–4.
(19) Bordel, D.; Putaux, J. L.; Heux, L. *Langmuir* **2006**, *22*, 4899–4901.
(20) Li, G.; Shi, L.; Ye, Q.; Zhou, W.; Tian, J. *Colloid Polym. Sci.* **2006**, *284*, 1179–1183.
(21) Price, C.; Deng, N.; Lloyd, F. R.; Li, H.; Booth, C. *J. Chem. Soc., Faraday Trans.* **1995**, *91*, 1357–1363.
(22) Sun, Z.; Wang, H. *Macromolecules* **1999**, *32*, 2605–2609.
(23) Wang, C. H.; Huang, Q. R. *J. Chem. Phys.* **1997**, *106*, 2819–2823.
(24) Berne, B. J.; Pecora, R. *Dynamic Light Scattering*; John Wiley & Sons: New York, 1976.
(25) Petzhold, C. L.; Stadler, R. *Macromol. Chem. Phys.* **1995**, *196*, 2625–2636.
(26) David, R. L. *Handbook of Chemistry and Physics*, 78th ed.; CRC Press: New York, 1997–1998.
(27) Young, C. Y.; Missel, P. J.; Mazer, N. A.; Benedek, G. B. *J. Phys. Chem.* **1978**, *82*, 1375–1378.
(28) Hiemenz, P. C. *Polymer Chemistry: The Basic Concepts*; Marcel Dekker: New York, 1984.
(29) Azzam, T.; Eisenberg, A. *Angew. Chem., Int. Ed.* **2006**, *45*, 7443–7447.
(30) Terreau, O.; Luo, L.; Eisenberg, A. *Langmuir* **2003**, *19*, 5601–5607.
(31) Burchard, W. *Cellulose* **2003**, *10*, 213–225.
(32) Boissy, C.; Allen, P.; Foulc, J. N. *J. Electrost.* **1995**, *35*, 13–20.
(33) Riegel, I. C.; Bittencourt, F. M.; Terrau, O.; Eisenberg, A.; Petzhold, C. L.; Samios, D. *Pure Appl. Chem.* **2004**, *76*, 123–131.

MA7023792